Clinics in Oncology

Case Report
Published: 30 Jul, 2016

Targeting RAGE Expression in Human Ovarian Cancer

Tekabe Y[1], Li Q[1], Rodriguez K[1], Johnson J[1], Khaw BA[2], Kokoshka J[3], Ray R[4], Rai V[4] and Johnson L[1]*

[1]Department of Medicine, Columbia University Medical Center, New York, USA

[2]Department of Pharmaceutical Sciences, Northeastern University, USA

[3]Department of Technology Ventures, Columbia University, New York, USA

[4]Institute of Life Sciences, Department of Biotechnology, Bhubaneswar, India

Abstract

Receptor for Advanced Glycation Endproducts (RAGE) is expressed in ovarian tissue and associated with ovarian carcinoma. With a radiolabeled anti-RAGE antibody, we proposed to show extent of RAGE expression in animal model and effect of blocking RAGE on ovarian cancer cell growth.

Methods: We measured inhibition of p-Akt and p-stat3 in SKOV-3 human ovarian carcinoma cell line and measured cell growth suppression in culture. For imaging, female nude mice (n = 15) at 6 wks of age were injected with luciferase expressing human ovarian cancer cells into the right flank. Four-five weeks later, animals were injected with luciferin and imaged on optical imager followed by injection with ^{111}In-anti-RAGE F(ab')$_2$ (n = 7) or ^{111}In-control IgG F(ab')$_2$ and 48 h later, were imaged on micro-SPECT/CT. Focal tracer uptake on scans was quantified, the tumors removed, radioactivity counted, and sectioned for histological and immunohistochemical examination.

Results: RAGE antibody pretreatment inhibited p-stat3 and p-AKT expression in SKOV-3 cells and there was a dose related reduction in cell growth in culture. There was good co-localization of the luciferase producing tumor on the optical scan and tumor location at necropsy with the focal uptake of the ^{111}In-anti-RAGE F(ab')$_2$. Quantitative tracer uptake in the tumor from scans showed that uptake of ^{111}In-anti-RAGE F(ab')$_2$ as %ID was 2.4 fold higher than ^{111}In-control F(ab')$_2$ (P = 0.01) confirmed by gamma well counting. Dual immunofluorescent staining for RAGE and PAX8 in tumors showed high expression of RAGE and co-localization with PAX8 positive stained cells.

Conclusion: RAGE expression in ovarian tumors in live animals can be imaged and quantified. An anti-RAGE F(ab')$_2$ used for imaging shows blocking properties and suppresses ovarian cancer cell growth.

Keywords: Ovarian cancer; RAGE; SPECT/CT Imaging

Introduction

Ovarian cancer is the fourth leading cause of cancer deaths in women [1]. Serum biomarker CA-125 is used to monitor the effects of ovarian cancer treatment, but is not accurate for detecting early disease [2]. Single-photon emission computed tomography/computed tomography (SPECT/CT) imaging with ^{111}In-satumomab pendetide (OncoScint) has limited diagnostic accuracy [3]. In biopsy and tissue samples paired-box gene 8 (PAX8) that encodes transcription factors associated with organogenesis, morphogenesis, thyroid, renal and Millerian cell differentiation and is highly expressed in ovarian cancer cells is used as a tissue marker [4]. Expression of Receptor for Advanced Glycated Endproducts (RAGE) in the tissue of reproductive human ovaries has been identified in multiple areas of ovarian dysfunction that make it a key component in identifying abnormalities similar to ovarian carcinoma [5] and is associated with the development of ovarian carcinoma [6]. RAGE is a multifunctional receptor binding a number of ligands known to play important roles in diabetes, atherosclerosis, cancer, and Alzheimer's disease [7-9]. The V domain on the extracellular RAGE receptor binds endogenous molecules referred to as damage associated molecular pattern molecules (DAMPs) that serve as ligands for RAGE, playing prominent roles in inflammation and cancer [10-13]. These ligands include proinflammatory cytokines S100 proteins, high-mobility group box 1 (HMGB1) proteins, and lysophosphatidic acid (LPA) [10-13]. The RAGE/ligand binding activates signaling pathways that enhance cell proliferation, activate pro-survival proteins, enhance autophagy, limit apoptosis, promote angiogenesis, and promote invasion and metastasis [14-21]. Cytoplasmic S100A4 expression is significantly stronger in ovarian cancers compared to

OPEN ACCESS

Correspondence:
Yared Tekabe, Department of Medicine, Columbia University Medical Center, New York, USA, Tel: 212-305-4275; Fax: 212-305-4648; E-mail: yt2166@columbia.edu

Received Date: *12 Jul 2016*
Accepted Date: *25 Jul 2016*
Published Date: *30 Jul 2016*

Citation:
Tekabe Y, Li Q, Rodriguez K, Johnson J, Khaw BA, Kokoshka J, et al. Targeting RAGE Expression in Human Ovarian Cancer. Clin Oncol. 2016; 1: 1055.

benign ovarian tumors, as well as being a strongly positive nuclear staining associated with poor prognosis [22]. The administration of s-RAGE, a soluble extracellular ligand-binding domain that acts as a decoy for RAGE ligands, or administration of an anti-RAGE antibody, blocked growth of C6 glioma cells engrafted into nude mice [23]. These findings indicate that blocking RAGE expression in ovarian cancer may suppress tumor growth. We developed a murine monoclonal anti-RAGE $F(ab')_2$ antibody fragment that binds a unique peptide sequence on the C-terminal of the V extracellular domain of RAGE. Using a ^{99m}Tc-labeled anti-RAGE $(Fab')_2$, we have shown uptake in atherosclerosis and peripheral artery disease in diabetes [24,25]. Furthermore, we have shown blocking properties of the antibody to suppress RAGE expression and thereby improve hind limb angiogenesis after femoral artery ligation in diabetic mice [26]. The present study extends our investigation into imaging and blocking antibody techniques on human SKOV-3 ovarian cancer cell line. We tested the effect of the antibody to change cell survival in culture and performed in-vivo imaging experiments using ^{111}In-labeled anti-RAGE $F(ab')_2$ and a small animal hybrid SPECT/CT imaging.

Materials and Methods

All animal studies were performed with the approval of the Institutional Animal Care and Use Committee of Columbia University.

Antibody

The antibody was developed against a unique peptide sequence on the V-domain of RAGE designed to display immunoreactivity in mice, pigs, and humans. Based on Genbank sequences, a peptide was prepared and used to immunize mice and subsequently hybridomas produced. Monoclonal antibodies (mouse IgG2a kappa) were produced in-vitro and purified by protein A and low endotoxin units (less than 3 endotoxin units/mg of purified antibody) (Strategic Diagnostics or SDIX, Newark DE). Monoclonal anti-RAGE $F(ab')_2$ fragments were developed as previously described [24].

Western blot analysis

SKOV-3 (Cell Biolabs, San Diego, CA) cells were maintained in DMEM medium supplemented with 10% fetal bovine serum (FBS) and 1% penicillin/streptomycin (Gibco-Life Technologies, Grand Island, NY) in a 5% CO_2 incubator at 37°C. For experiments, cells were plated at a density of 1x 10^5 cells/ml in 60 mm dish. Cells were serum starved for overnight after they reached 70-80% confluency and next day cells were pre-treated with 50 μg/ml IgG or anti-RAGE Fab for one hour followed by treatment with 10 μg/ml of AGEs for 20 minutes. Tumor cells were lysed and total cell lysates were immunoblotted and probed with RAGE, p-AKT, AKT, p-stat3 and stat3 antibodies (Cell Signaling (Danvers, MA). Briefly, protein (35 μg) from cell lysates were denatured, resolved by 10% acrylamide gels and transferred to a nitrocellulose membrane. Membranes were blocked in 5% non-fat dry milk and then incubated with primary antibodies: p-AKT, p-stat3, RAGE. HRP-conjugated anti-rabbit IgG and anti-mouse (Amersham, Piscataway, NJ) was used to identify sites of primary antibody binding. Membranes were stripped of bound primary antibodies and re-probed with total AKT, total stat-3 and β-actin antibodies. The ratios (phospho/total) were quantified and normalized using ImageJ software (NIH, Bethesda, MD, USA).

Cell viability assay

SKOV-3s (paclitaxel-sensitive) and SKOV-3TR (paclitaxel-resistant) cell lines were used in cell culture experiments. Briefly, cells were plated (4000 cells/well) in to 96 well plates and maintained at 37°C for 24 hours (h) in a humidified incubator with 5% CO_2. Media was removed and serial dilutions of anti-RAGE antibody or control antibody was added to the plates: 50, 25, 12.5, 6.25, 3.125, 1.562, 0.781 μg/ml. Plates were incubated for 24 h at 37°C and 5% CO_2 then washed with respective media. CellTiter Blue (Promega, Madison, WI) (50μl of 1:5 dilutions) was added to plates and incubated at 37°C and 5% CO_2 for around 2 h. Fluorescence was recorded (excitation, 560 nm: emission, 590 nm) using BioTek Fluorescence Plate Reader.

Animals

Female nude (J:NU) mice (6-7 wks of age) were purchased from The Jackson Laboratories (Indianapolis, IN). Mice were injected subcutaneously with luciferase producing SKOV-3 cells (3 x 10^6 cells in 0.1 ml PBS) (n = 13) into the right flank, Tumor sizes on the flanks were measured weekly with calipers and calculated as: (length x height x width x π)/6 [27,28]. Imaging experiments were performed when tumor reached 1070±279 mm^3, occurring 4-5 w ks after tumor injection.

Radiotracer preparation

For ^{111}In labeling, approximately 1 mg of the $F(ab')_2$ in 0.1 M $NaHCO_3$ buffer (pH 8.2) was conjugated with a 5 molar excess of [(R)-2-Amino-3-(4-isothiocyanatophenyl)propyl]-trans-(S,S)-cyclohexane-1,2-diamine-pentaacetic acid (*p*-SCN-Bn-CHX-A"-DTPA; Macrocyclics). The reaction mixture was incubated at room temperature for 1 h followed by overnight dialysis at 4°C in 0.25 M NH_4Ac (pH 5.5). To 10 μl (74 - 111 MBq) (2-3 mCi) of ^{111}In in 0.05 N HCl, 5 volumes of 0.1 M NH_4Ac (pH 5.5) was mixed and after 10 min, 50 μl (50 μg) of DTPA conjugated anti-RAGE $F(ab')_2$ was added. The reaction mixture was incubated at room temperature for 45 min. ^{111}In-labeled antibody fragments were separated from free ^{111}In using PD 10 column pre-equilibrated with 0.1 M NH_4Ac (pH 6). The mean specific activity was 7.65 ± 0.75 MBq/μg of protein, and the mean radiopurity was 97.7 ± 0.95% by instant thin-layer chromatography.

Biodistribution and blood pool clearance

Five tumor implanted nude mice were used to measure biodistribution of ^{111}In-anti-RAGE $(Fab')_2$. Each animal was euthanized by an intraperitoneal injection of pentobarbital (100 mg/kg). Organs were dissected, weighed, and counted in a gamma counter (Wallac Wizard 1470, PerkinElmer, Waltham, MA, USA) for determination of the percent injected dose of radiotracer per gram (%ID/g) tissue. Radiotracer activity in the samples was corrected for background, decay time, and tissue weight. To determine optimal imaging time, 3 mice were euthanized at 24 and 48 h after tracer injection and tissue samples of the tumor and blood counted. At 24 h, the ratio of tumor/blood = 0.18 and at 48 h the ratio was 2.7 and therefore 48 h time point was selected for imaging.

Imaging

Mice underwent micro-SPECT/CT (Bioscan/Mediso) imaging 48 h after tracer injection. Prior to SPECT imaging the mice underwent bioluminescence imaging to detect the signal from the luciferase producing tumor cells. Mice were anesthetized and injected IP with luciferin (150 μg in 100 μl/mouse). Twenty min later, mice were imaged using a PhotonImager optical imaging device (Biospace lab, Paris, France). Light emission was detected by an ICCD camera and quantified using image processing M3 Vision software (Biospace lab). Following optical imaging, 4.81 ± 1.11 MBq (0.13 ± 0.03 mCi)

^{111}In-anti-RAGE F(ab')$_2$ was injected via the femoral vein catheter. Forty-eight h later, mice were imaged on a nano-SPECT/CT scanner (Bioscan, Washington DC). A topogram (sequence of 2D side view x-ray projections) was used to determine the axial scan range for SPECT and CT imaging. CT images were acquired with an integrated CT scanner using an x-ray tube at 45 kVp and an exposure time of 1000 ms per view. Following CT acquisition, helical SPECT scans were acquired using dual-headed detectors each outfitted with collimators with nine pinholes. Each pinhole had a diameter of 1.4 mm providing a transaxial field-of-view (FOV) of 30 mm and an axial FOV of 16 mm, extendable through helical scanning to 270 mm. SPECT data were acquired with the following parameters: step and shoot rotation, 30° step in 360° rotation using 24 projections, 60 s per projection, 256 x 256 frame size with 1.0 mm pixels, and 140 keV with 10% energy window. The projection data were reconstructed by OSEM algorithm with subset and iteration number set to 16 and 8, respectively, and a voxel size of 300 µm and SPECT and CT datasets fused. At the completion of *in-vivo* imaging, the animals were sacrificed and tumors were harvested, radioactivity counted, and fixed in 10% formalin.

Image analyses

Regions of interest (ROIs) with equal voxel thickness were drawn on transaxial slices that comprised the tumor volume identified from the CT scan. Uptake of ^{111}In-anti-RAGE F(ab')$_2$ in the tumor was quantified as MBq (mCi) using a calibration factor determined from mouse-shaped phantoms filled with known levels of ^{111}In imaged with the same protocol and entered into the display software (*In vivo* Scope software). The tumor uptake from the scans was divided by the total injected dose to obtain percent injected dose (%ID).

Gamma well counting

Tumors were weighed and the radiotracer uptake was determined in a gamma well counter (Wallac Wizard 1470, PerkinElmer) and expressed as the percentage injected dose per gram (%ID/g) of tissue. The radiotracer activity in the samples was corrected for background, decay time, and tissue weight.

Histopathology

The explanted tumors were fixed in 10% formalin for 24 h followed by 70% alcohol awaiting decay followed by paraffin embedding. Serial sections (5-µm-thick) from paraffin-embedded tumors were processed for hematoxylin and eosin (H&E) for morphological evaluation and immunohistochemical characterization. Serial sections were deparaffinized and rehydrated followed by quenching of endogenous peroxidase activity with 0.3% hydrogen peroxide. Slides were then incubated overnight with primary antibody for RAGE (50 µg/ml; mouse anti-RAGE F(ab')$_2$ and anti-Paired-box gene 8 (PAX;1:100). Slides were incubated for 30 min with biotinylated respective secondary antibodies. Sections were treated for 30 min with VECTASTAIN ABC reagent (Vector Laboratories). Color reaction was visualized with 3',3'-diaminobenzidine (DAB substrate kit, Dako) and counterstained with Gill's hematoxylin solution. Images were captured using a digital camera mounted on a Nikon microscope and analyzed using Image-Pro Plus software (Media Cybernetics Inc., Bethesda, MD).

Immunofluorescence

Dual fluorescent confocal microscopy studies were performed to co-localize RAGE with PAX8 positive cells and macrophages. Briefly, tumor sections were incubated with anti-RAGE F(ab')$_2$ (Texas red;

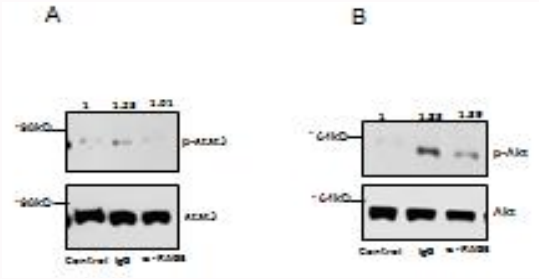

Figure 1: Levels of (A) phosphorylated/total stat3 and (B) phosphorylated Akt (Ser473)/total Akt in SKOV-3 cells shown by western blotting upon stimulation with 10 µg/ml of AGEs for 20 minutes after treatment with 30 µg/ml of control F(ab')$_2$ or α-RAGE F(ab')$_2$.

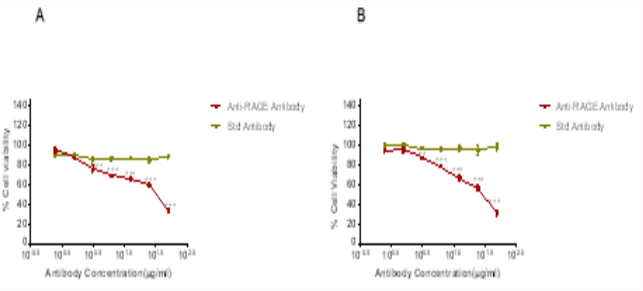

Figure 2: Cell viability assay. Cell viability of SKOV-3 paclitaxel-sensitive (A) and paclitaxel-resistant SKOV-3 (B) cells after treatment with anti-RAGE F(ab')$_2$ or with control F(ab')$_2$. P < 0.01** and *P* < 0.001***.

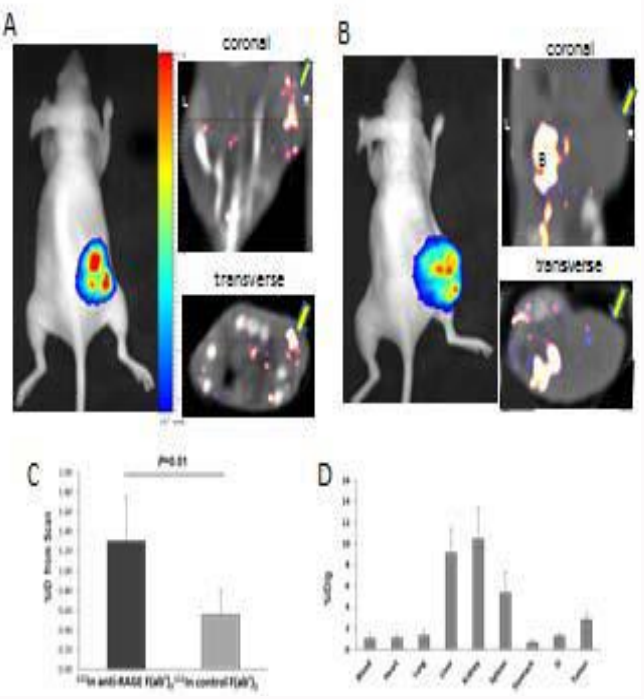

Figure 3: (A) Bioluminescent image on left of nude mouse engrafted in left flank with luciferase producing SKOV-3 cells and coronal, and on right transverse SPECT/CT images obtained from same mouse injected with ^{111}In-anti-RAGE F(ab')$_2$ showing focal tracer uptake in left flank. (B) Same format as A for mouse injected with and ^{111}In-control F(ab')$_2$ showing minimal tracer uptake in the left flank. (C) Graph showing quantitative tracer uptake as %ID for ^{111}In labeled anti-RAGE ab and labeled inactive probe. (D) Biodistribution of ^{111}In-anti-RAGE F(ab')$_2$ in tumor and non-tumor organs in female nude mice engrafted with SKOV-3 cells. B=Bladder.

1:100) and co-stained with anti-PAX antibody (FITC; 1:50) or anti-macrophage (1:50, Santa Cruz). The images were examined using a fluorescence microscope (Nikon).

Statistical analyses

Comparisons between groups were made using the Student *t* test. All statistical tests were two-tailed, with $P < 0.05$ denoting significance. The cell viability assay data were analyzed with two-way ANOVA and the Bonferroni multiple comparison tests.

Results

Western blot analysis

Western blot analysis demonstrated a reduction of p-AKT (Ser473) in SKOV-3 cells pretreated with 10 μg/ml of anti-RAGE $F(ab')_2$ compared to cells pretreated with control IgG $F(ab')_2$. RAGE antibody fragment pretreatment inhibited p-stat3 and p-AKT expression by 99.9% and 53%, respectively (Figure 1).

Cell viability assay

The effects of increasing doses of anti-RAGE antibody on human ovarian cancer cell lines: SKOV-3s (paclitaxel-sensitive) and SKOV-3TR (paclitaxel-resistant) are shown in (Figure 2A and B), respectively. At 50 μg/ml dose, the anti-RAGE antibody significantly lowered the % cell viability of both ovarian cancer cell lines in a dose-responsive manner as compared to the negative control ($P < 0.001$).

Tumor grafts in nude mice

Macroscopically, tumor-bearing mice developed palpable masses at the region of implantation with a mean tumor volume of 1070±279 mm^3.

In-vivo imaging

Bioluminescent imaging on an optical imager (BioSpace Lab, Paris, France) showed signal from luciferase producing SKOV-3 cells in the flank where the tumors were grafted. The SPECT/CT imaging of the uptake of ^{111}In-anti-RAGE $F(ab')_2$ showed uptake of radiolabeled antibody fragment that co-localized to the optical signal from the luciferase producing tumor cells (Figure 3A). Non immune control antibody fragment showed minimal uptake at the target (Figure 3B).

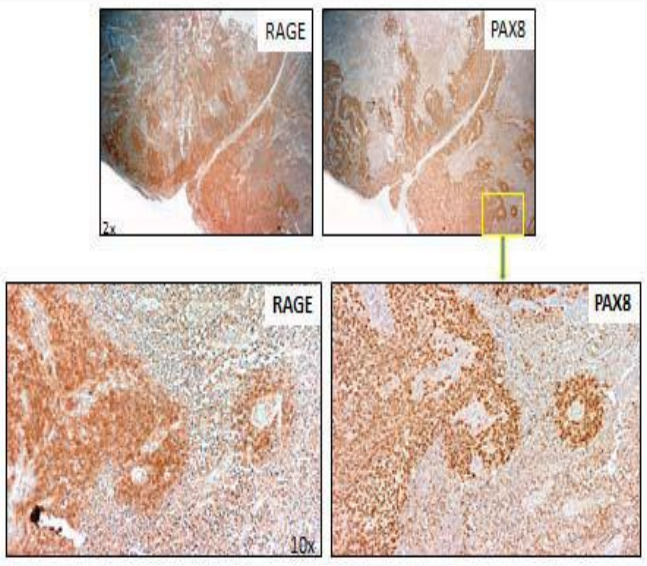

Figure 4: Immunohistological sections at 20x (top) and 100X (lower) from explanted tumors with secondary HRP (brown chromogen) stain showing expression of RAGE that corresponds to staining for SKOV-3 antigen PAX8.

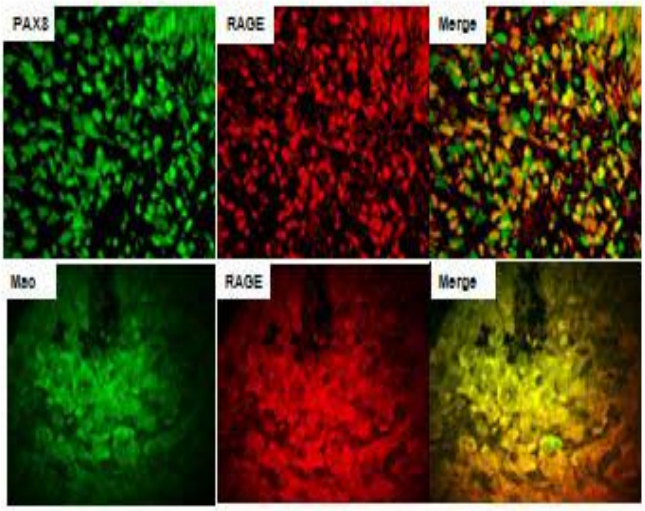

Figure 5: Dual fluorescent confocal microscopic images from SKOV-3 tumor sections. The top row shows dual immunofluorescent staining for RAGE (red) and PAX8-positive cells (green) show colocalization in the merged image (yellow). The bottom row shows colocalization of Macrophage staining with RAGE. Magnification x400.

Quantitative tracer uptake in tumors

The quantitative accumulation of ^{111}In-anti-RAGE $F(ab')_2$ in the tumor from the scan (1.3 ± 0.45% ID) was significantly higher than the uptake of ^{111}In-control $F(ab')_2$ (0.56 ± 0.25, P=0.01) (Figure 3C). The higher uptake of ^{111}In-anti-RAGE $F(ab')_2$ in the tumor was confirmed by *ex-vivo* gamma counting. There was a significantly greater tumor uptake of ^{111}In-anti-RAGE $F(ab')_2$ (2.86 ± 0.57% ID/g) compared with ^{111}In-control $F(ab')_2$ (0.52± 0.21%; $P < 0.001$).

Tracer biodistribution

Accumulation of ^{111}In-anti-RAGE $F(ab')_2$ in non-target organs is shown in (Figure 3D). The liver and kidneys had the highest accumulation uptake of tracer.

Histopathology

Immunohistochemical staining of the explanted tumor sections revealed RAGE visually co-localized with sites of PAX8-positive cells (Figure 4). Dual immunofluorescent staining confirmed co-localization of RAGE with PAX8 and also with macrophages (Figure 5).

Discussion

We showed that a radiolabeled anti-RAGE antibody fragment targeting luciferase producing ovarian tumors co-localizes with the luciferase signal on optical imaging and can be visualized on SPECT/CT scans and correlates with immunohistology. By Western blot analysis, we showed that our antibody has blocking properties based on a marked reduction of p-AKT (Ser473) in SKOV-3 cells pretreated with anti-RAGE antibody $F(ab')_2$ and that exposing these cancer cells in culture to the antibody, growth is reduced. Immunohistochemistry and dual fluorescence staining reported in this paper show RAGE co-localized with PAX stain for the paired box growth gene expressed in tumor cells and also with Mac stain identifying macrophages. Together, these two co-localizing stains document the role of RAGE in pathways of inflammation and tumor genesis. DAMPs include ligands that are released in the setting of cellular stress, damage,

inflammation, or necrotic cell death bind to receptors that activate immune responses or tissue repair. The same process in addition to being beneficial can lead to chronic inflammation and neoplastic transformation or contribute to the inflammation induced by primary neoplasia leading to tumor growth and metastasis [11,12]. Currently, there are few imaging strategies that identify ovarian cancer in its early stage. Satumomab pendetide (OncoScint) is an IgG murine monoclonal antibody that targets the cell surface mucin-like glycoprotein antigen TAG-72 found on colorectal and ovarian cancers. The antibody labeled with ^{111}In has been in clinical use for more than 10 years. While its sensitivity for detecting cancer spread in the abdomen is better than CT, it is not sensitive for detecting early disease [3]. In addition, since it is a murine antibody, about 40% of patients develop human anti-mouse antibody levels after injection. For further imaging and treatment, we have humanized our anti-RAGE antibody which would eliminate reactions to mouse antigens. High liver uptake as shown in our biodistribution data is common in radiolabeled antibodies and is a limitation for nuclear imaging of intra-abdominal malignancies. Potentially more important clinically than development of an ovarian cancer imaging tracer is development of a RAGE suppressing treatment agent in ovarian cancer. RAGE expression is increased and downstream pathways activated by RAGE ligands. Two classes of RAGE ligands or DAMPs - S100 and HMGB1 proteins - have been found in a number of tumors [14-17]. While S100 proteins are localized in the cytoplasm, HMGB1 is localized to the nucleus gaining access to bind nuclear membranes on tumor cells undergoing necrosis [16]. The intracellular signaling pathways, initiated by RAGE/HMGB1 binding in tumors, promote proliferation and invasion of tumor cells via several pathways. In-vitro binding studies have identified a cytoplasmic region of RAGE as an ERK docking site [21]. A recently reported additional ligand binding RAGE and stimulating tumor growth is LPA (lysophosphatidic acid) which regulates fundamental cellular processes such as proliferation, survival, motility and invasion [18]. Reported studies using tissue microarrays have documented RAGE expression in several human tumors. In particular, RAGE expression has been shown in human ovarian cancer cells and the ligands S100A4, S100AI4, HMGB2 overexpressed and secreted by ovarian carcinoma cells [22]. S100 ligands, low molecular weight proteins able to form homodimers and heterodimers and oligomers have a variety of functions in cell growth and members of the family have been shown to change the microenvironment favoring tumor metastasis [15]. Cytoplasmic S100A4 expression is significantly stronger in ovarian cancers compared to benign ovarian tumors and strongly positive nuclear staining is associated with poor prognosis [22]. The RAGE gene is found on chromosome 6p21.3 in the major histocompatibility locus (MHC). Polymorphisms at the RAGE gene locus was identified in 1998 [31]. Population based studies have investigated single nucleotide polymorphisms (SNPs) have recently focused on investigating functional polymorphisms in the RAGE gene that may affect the expression or function of RAGE and are associated with certain malignancies. One polymorphism was found to be a significant factor in several malignancies including ovarian cancer [32,33]. This SNP designated 82G/S codes for a change from glycine to serine within the putative ligand-binding domain of the receptor protein [31,32]. Specific mechanisms to link this change in the ligand-binding domain and carcinogenesis are not yet been worked out but in light of interest in personalized medicine identifying a target such as RAGE with a genetic variant in the RAGE gene linked to carcinogenesis and important role of RAGE in some specific tumors makes RAGE a potential target for identifying at risk patients for higher surveillance possibly involving imaging and for treatment strategies to reduce RAGE expression.

Summary and Future Directions

This current study is the first to report that a radiolabeled antibody against RAGE localizes to ovarian cancer cells injected into nude mice and can be imaged in live animals on SPECT/CT. The important role of RAGE expression and binding of ligands that activate many pathways necessary for tumor growth and metastasis indicate that RAGE expression is a key biological tumor marker. In addition, the antibody we developed has blocking properties that can inhibit tumor cell growth in culture. Further work is needed to demonstrate effect of treatment with antibody to inhibit tumor growth in mice.

References

1. Berchuck A, Schildkraut JM, Marks JR, Futreal PA. Managing hereditary ovarian cancer risk. Cancer. 1999; 86: 2517-2524.
2. Bast RC, Klug TL, St. John E, Jenison E, Niloff JM, Lazarus H, et al. A radioimmunoassay using a monoclonal antibody to monitor the course of epithelial ovarian cancer. New England Journal of Medicine. 1983; 309: 883-887.
3. Pinkas L, Robins PD, Forstrom LA, Mahoney DW, Mullan BP. Clinical experience with monoclonal antbodies in detection of colorectal and ovarian cancer recurrence and review of the literature. Nucl Med Commun. 1999; 20: 689-696.
4. Liliac L, Carcangiu ML, Canevari S, Amălinei C. The value of PAX8 and WT1 molecules in ovarian cancer diagnosis. Rom J Morphol Embryol. 2013; 54: 17-27.
5. Merhi Z. Advanced glycation end products and their relevance in female reproduction. Hum Reprod. 2014; 29: 135-145.
6. Diamanti-Kandarakis E, Piperi C, Patsouris E, Korkolopoulou P, Panidis D, Pawelczyk L, et al. Immunohistochemical localization of advanced glycation end-products (AGEs) and their receptor (RAGE) in polycystic and normal ovaries. Histochem Cell Biol. 2007; 127: 581-589.
7. Bucciarelli LG, Wendt T, Rong L, Lalla E, Hofmann MA, Goova MT, et al. RAGE is a multiligand receptor of the immunoglobulin superfamily: implications for homeostasis and chronic disease. Cell Mol Life Sci. 2002; 59: 117-1128.
8. Yan SF, D'Agati V, Schmidt AM, Ramasamy R. Receptor for Advanced Glycation Endproducts (RAGE): a formidable force in the pathogenesis of cardiovascular complications of diabetes and aging. Curr Mol Med. 2007; 7: 699-710.
9. Yan SF, Ramasamy R, Schmidt AM. Mechanisms of disease: advanced glycation endproducts and their receptor in inflammation and diabetes complications. Nat Clin Pract Endocrinol Metab. 2008; 4: 285-293.
10. Srikrishna G, Freeze HH. Endogenous damage-associated molecular pattern molecules at the crossroads of Inflammation and cancer. Neoplasia. 2009; 11: 615-628.
11. Sparvero LJ, Asafu-Adjei D, Kang R, Tang D, Amin N, Im J, et al. RAGE (Receptor for Advanced Glycation Endproducts), RAGE Ligands, and their roles in Cancer and Inflammation. J Transl Med. 2009; 7: 17.
12. Logsdon, CD, Fuentes MK, Huang EH, Arumugam T. RAGE and RAGE ligands in cancer. Curr Mol Med. 2007; 7: 777-789.
13. Rojas A, Figueroa H, Morales E. Fueling inflammation at tumor microenvironment: the role of multiligand/RAGE axis. Carcinogenesis. 2010; 31: 334-341.
14. Hoffman MA, Drury S, Fu C, Qu W, Taguchi A, Lu Y, et al. RAGE mediates a novel proinflammatory axis: a central cell surface receptor for

S100/calgranulin polypeptides. Cell. 1999; 97: 889-901.

15. Hsieh HL, Schafer BW, Sasaki N, Heizmann CW. Expression analysis of S100 proteins and RAGE in human tumors using tissue microarrays. Biochem Biophys Res Commun. 2003; 307: 375-381.

16. Kostova N, Zlateva S, Ugrinova I, Pasheva E. The expression of HMGB1 protein and its receptor RAGE in human malignant tumors. Mol Cell Biochem. 2010; 337: 251-258.

17. Ellerman JE, Brown CK, deVera M, Zeh HJ, Billiar T, Rubartelli A, et al. Masquerader: high mobility group box-1 and cancer. Clin Cancer Res. 2007; 13: 2836-2848.

18. Rai V, Touré F, Chitayat S, Pei R, Song F, Li Q, et al. Lysophosphatidic acid targets vascular and oncogenic pathways via RAGE signaling. J Exp Med. 2012; 209: 2339-2350.

19. Kang R, Tang D, Schapiro NE, Livesey KM, Farkas A, Loughran P, et al. The receptor for advanced glycation end products (RAGE) sustains autophagy and limits apoptosis, promoting pancreatic tumor cell survival. Cell Death Differ. 2010; 17: 666–676.

20. Kuniyasu H, Oue N, Wakikawa A, Shigeishi H, Matsutani N, Kuraoka K, et al. Expression of receptors for advanced glycation end-products (RAGE) is closely associated with the invasive and metastatic activity of gastric cancer. J Pathol. 2002; 196: 163-170.

21. Malik P, Chaudhry N, Mittal R, Mukherjee TK. Role of receptor for advanced glycation end products in the complication and progression of various types of cancers. Biochim Biophs Acta. 2015; 1850; 1898-1904.

22. Kikuchi N, Horiuchi A, Osada R, Imai T, Want C, Chen X, et al. Nuclear expression of S100A4 is associated with aggressive behavior of epithelial ovarian carcinoma: an important authocrine/paracrine factor in tumor progression. Cancer Sci. 2006; 97: 1061-1069.

23. Taguchi A, Blood DC, del Toro G, Canet A, Lee DC, Qu W, et al. Blockade of RAGE-amphoterin signaling suppresses tumour growth and metastases. Nature. 2000; 18: 354-360.

24. Tekabe Y, Li Q, Rosario R, Sedlar M, Majewski S, Hudson BI, et al. Development of receptor for advanced glycation end products-directed imaging of atherosclerotic plaque in a murine model of spontaneous atherosclerosis. Circ Cardiovasc Imaging. 2008; 1: 212-219.

25. Tekabe Y, Shen X, Luma J, Weisenberger D, Yan SF, Haubner R, et al. Imaging the effect of receptor for advanced glycation endproducts on angiogenic response to hindlimb ischemia in diabetes. EJNMMI Res. 2011; 1: 3.

26. Tekabe Y, Anthony T, Li Q, Ray R, Rai V, Zhang G, et al. Treatment effect with anti-RAGE F(ab')2 antibody improves hind limb angiogenesis and blood flow in Type 1 diabetic mice with left femoral artery ligation. Vasc Med. 2015; 20: 212-218.

27. Connolly DC, Hensley HH. Xenograft and transgenic mouse models of epithelial ovarian cancer and non invasive imaging modalities to monitor ovarian tumor growth in situ- applications in evaluating novel therapeutic agents. Curr Protoc Pharmacol. 2009; 45: 14.

28. Tomayko MM, Reynolds CP. Determination of subcutaneous tumor size in athymic (nude) mice. Cancer Chemother Pharmacol. 1989; 24: 148-154.

29. DiNorcia J, Moroziewicz DN, Ippagunta N, Lee MK, Foster M, Rotterdam HZ, et al. RAGE signaling significantly impacts tumorigenesis and hepatic tumor growth in murine models of colorectal carcinoma. J Gastrointest Surg. 2010; 14: 1680-1690.

30. Tateno T, Ueno S, Hiwatashi K, Matsumoto M, Okumura H, Setoyama, et al. Expression of receptor for advanced glycation end products (RAGE) is related to prognosis in patients with esophageal squamous cell carcinoma. Ann Surg Oncol. 2009; 16: 440-446.

31. Hudson BI, Strickland MH, Grant PJ. Identification of polymorphisms in the receptor for advanced glycation end products (RAGE) gene: prevalence in type 2 diabetes and ethnic groups. Diabetes. 1998; 47: 1155-1157.

32. Xia W, Xu Y, Mao Q, Dong G, Shi R, Wang J, et al. Association of RAGE polymorphisms and cancer risk: a meta-analysis of 27 studies. Med Oncol. 2015; 32: 442.

33. Zhang S, Hou X, Zi S, Wang Y, Chen L, Kong B. Polymorphisms of receptor for advanced glycation end products and risk of epithelial ovarian cancer in Chinese patients. Cell Physiol Biochem. 2013; 31: 525-531.